International Journal of Metallurgical &
Materials Science and Engineering (IJMMSE)
ISSN(P): 2278-2516; ISSN(E): 2278-2524
Vol. 7, Issue 2, Apr 2017, 7-28

Original Article

MOLECULAR STRUCTURE, VIBRATIONAL SPECTRA, UV–VIS, NBO, AND NMR ANALYSES ON POTASSIUM 2-[2-(2, 6-DICHLOROANILINO) PHENYL] ACETATE USING AB INITIO DFT METHODS

J. DANIEL KISSINGER & S. STELLA MARY

Department of Physics, St. Peter's University, Avadi, Chennai, Tamil Nadu, India

ABSTRACT

In this work, FT-IR and FT-Raman spectra of potassium 2-(2-(2,6-dichlorophenylamino)phenyl)acetate (abbreviated as K2DCPAPA) have been reported in the regions 4000–450 cm^{-1} and 4000–50 cm^{-1}, respectively.CAM-B3LYP/6-31G(d,p) and HF/6-31G(d,p) calculations were performed to obtain the optimized molecular structures, vibrational frequencies and corresponding vibrational assignment, thermodynamic properties and natural bonding orbital (NBO) analysis. A detailed interpretation of the vibrational spectra of this compound has been made on the basis of the calculated Potential Energy Distribution (PED). The calculations of the electronic spectra were compared with the experimental ones. The time dependent DFT method employed to study its absorption energy and oscillator strength. The calculated HOMO and LUMO energy reveals shows that the charge transfers occurring within the molecule. Stability of the molecule arising from hyper conjugative interaction, charge delocalization has been analyzed using natural bond orbital (NBO) analysis. The electronic properties, such as HOMO and LUMO energies, molecular electrostatic potential (MESP) were also performed. The study is extended to the HOMO - LUMO analysis to calculate the energy gap (Δ), Ionization potential (I), Electron Affinity (A), Global Hardness (η), Chemical Potential (μ), Global Electrophilicity (w). Non-linear optical NLO behavior of the examined molecule was investigated by the determination of the electric dipole moment, the polarizability and the hyperpolarizability using the CAM-B3LYP and HF with 6-31G(d,p) basis set. The isotropic calculated chemical shifts computed by ^{13}C and ^{1}H NMR analysis also show good agreement with Chemsoft Ultra values. The First order Hyperpolarizability (β) and Molecular Electrostatic Potential (MESP) of the molecule was computed using DFT calculations.

KEYWORDS: CAM-B3LYP, FT-IR, FT-Raman, K2DCPAPA & HOMO LUMO

Received: Mar 16, 2017; **Accepted:** Apr 05, 2017; **Published:** Apr 12, 2017; **Paper Id.:** IJMMSEAPR20172

INTRODUCTION

Diclofenac is a non steroidal anti-inflammatory drug (NSAID) taken or applied to reduce inflammation and as an analgesic reducing pain in certain conditions. The name "diclofenac" derives from its chemical name: 2-(2-(2,6-dichlorophenylamino)phenyl)acetate. Diclofenac was first synthesized by Alfred Sallmann and Rudolf Pfister and introduced as Voltaren by Ciba-Geigy (now Novartis) in 1973 [1]. In the United Kingdom, United States, India, and Brazil diclofenac may be supplied as either the sodium or potassium salt; in China, it is most often supplied as the sodium salt, while in some other countries it is only available as the potassium salt. It is available as a generic drug in a number of formulations, including diclofenac diethyl amine, which is applied topically. The drug's use in animals is controversial due to its toxicity which can rapidly kill scavenging birds that may eat dead animals. It has been banned for veterinary use in many countries. Inflammatory disorders may include musculoskeletal complaints, especially osteoarthritis, dental

pain, temporomandibular joint (TMJ) pain, spondylarthritis, ankylosing spondylitis, gout attacks, [2] and pain management in cases of kidney stones and gallstones. An additional indication is the treatment of acute migraines. Diclofenac is used commonly to treat mild to moderate postoperative or post-traumatic pain, in particular when inflammation is also present, and is effective against menstrual pain and endometriosis. It is used to relieve pain and swelling (inflammation) from various mild to moderate painful conditions.

Density functional theory (DFT), as it is used for computational chemistry, the hybrid functional B3LYP appears to offer the greatest contribution. However, it is unsuccessful in a number of important applications: (i) the polarisability of long chains, (ii) excitations using time dependent theory (TD-DFT) for Rydberg states and perhaps most important (iii) charge transfer excitations. To rectify this fact, Y anai et al. explained that CAM-B3LYP is the best method in their paper. In the present study, the molecular structures were calculated by using CAM-B3LYP/6-31G(d,p) and HF/6-31G(d,p) calculation levels and were compared with the experimental results. The aim of the work is to investigate the molecular structure, vibrational spectra, frontier molecular orbital, Natural bond orbital (NBO) analysis and NLO properties of the title molecule due to its pharmaceutical importance been analyzed by density functional theory (DFT) and Hartree Fork (HF) methods in the basis set 6-31G(d,p).

EXPERIMENTAL METHODS

The compound K2DCPAPA (99%) was purchased from Sigma-Aldrich Company and used as such for the spectral measurements. The room temperature Fourier Transform IR spectra of the title compounds were measured in the 4000-450 cm^{-1} region at a resolution of $\pm 2cm^{-1}$ using BRUKER Tensor 27 FT-IR spectrometer equipped with a KBr beam splitter and globar source. The Fourier Transform-Raman spectra of K2DCPAPA were recorded on a BRUKER IFS-66 V model interferometer equipped with an FRA-106 FT-Raman accessory. The spectra were recorded in the region 4000-$50cm^{-1}$ stokes region using the 1064nm line of Nd: YAG laser for the excitation operating at 200mW power. The reported wave numbers were expected to be accurate within $\pm 2cm^{-1}$.

COMPUTATIONAL DETAILS

The molecular geometry optimization and vibrational frequency calculations were carried out for glutamic acid, with GAUSSIAN 09W software package [3] Coulomb attenuating method – Becke's three parameter exchange functional (B3),[4,5] and combined with the correlation functions of Lee, Yang and Parr (LYP) [6] combined with standard 6-31G(d,p) basis set. The atomic charges, electric dipole moment, HOMO, LUMO and other thermodynamic parameters were also calculated theoretically. A newly designed functional, the long range Coulomb-attenuating method (CAM-B3LYP) considered long-range interactions comprising 19% of HF and 81% of B88 exchange at short range and 65% of HF plus 35% of B88 at long range [7] and to the best of our knowledge, double hybrid methods used for the first time to compare with the CAM-B3LYP method. The combination of HF and B88 is a better method than the double hybrid method, so that we used the CAM-B3LYP method in our work. DFT calculations are reported to provide excellent vibrational frequencies of organic compounds if the calculated frequencies are scaled to compensate for the approximate treatment of electron correlation for the basis set deficiencies and for the an harmonicity. [8–10].

RESULTS AND DISCUSSIONS

Molecular Geometry

The optimised geometrical parameters of glutamic acid calculated by the CAM-B3LYP/6-31G(d,p) and HF/6-31G(d,p) methods are listed in Table 1 in accordance with the atom numbering scheme given in Figure 1. From the structural data given in Table 1, It is observed that the various bond lengths, bond angles and bond dihedral angles are found to be almost same at the CAM-B3LYP/6-31G(d,p) and HF/6-31G(d,p) level of theory. Molecular geometries can be specified in terms of bond lengths, bond angles and bond dihedral angles. It can be inferred that the bond be stronger, the overlap should be greater, which in turn would shorten the distance between the nuclei, i.e. bond length. A shorter length for K2DCPAPA, the strongest bonds are formed between H(27)-N(12)= 1.0284 A° (CAM-B3LYP/6-31G(d,p)) and H(27)-N(12)= 1.0018 A°(HF/6-31G(d,p)) having small bond distance compared to others and the weakest bond is Cl(20)-K(1) 3.2605 A having a very high bond distance (Cl(20)-K(1) (3.2605 A°) as computed by the CAM-B3LYP/6-31G(d,p) method. The calculated geometric parameters can be used as foundation to calculate the other parameters for the compound. The calculated geometrical parameters were compared with X-ray diffraction results. [11] The X-ray data and calculated geometric parameters fairly agrees with almost all values. The small deviations are probably due to the intermolecular interactions in the crystalline state of the molecule. The bond angle between C(6)-C(5)-C(4) by HF and CAM-B3LYP are calculated to be 120.1° and 120° which agrees with the experimental value of 120°. The bond angle between C(7)-C(2)-C(3) by HF and CAM-B3LYP methods are 119.6° and 119.7° respectively, which is in good agreement with experimental values of 120°. The calculated dihedral angles H(24)-C(7)-C(2)-C(3)179.2 and C(5)-C(4)-C(3)-N(12) (179.9) show good agreement with X-ray diffraction results (180.0) and (180.0), respectively, for the above dihedral angles and it reveals that the structure is coplanar.

VIBRATIONAL ANALYSIS

The experimental FT-IR and calculated vibrational spectra are shown in Figures 2 and 3, FT-Raman and calculated spectra are shown in Figure 4 and 5. The observed and calculated frequencies using CAM-B3LYP/6-31G(d,p) and HF/6-31G(d,p) methods with IR intensity and probable assignment of K2DCPAPA are summarised in Table 2.

C=O STRETCHING

The carbonyl stretching frequency has been most extensively studied by IR spectroscopy [12] and it is highly characteristic with intense absorption. This multiple-bonded group is highly polar and therefore gives rise to an intense IR absorption band. The carbon–oxygen double bond is formed by bonding between carbon and oxygen internal hydrogen bonding. It reduces the frequencies of the C=O stretching absorptions to a greater degree than by inter molecular H bonding; because of the different electro negativity of C and O, the bonding is not equally distributed between the two atoms. Normally carbonyl group vibrations occur in the region 1850–1600 cm^{-1}. [13] In our study, the theoretically computed HF/6-31G(d,p) value1820 cm^{-1} and CAM-B3LYP/6-31G(d,p) method value 1708 cm^{-1} are assigned to C=O stretching vibration. A very strong band observed in the FT-IR spectrum at 1798 cm^{-1} are assigned to C=O stretching vibrations. This C=O vibration appearing in the expected range shows that it is not much affected by other vibrations.

C-H VIBRATIONS

The hetroaromatic organic compound and its derivatives are structurally very close to benzene and commonly exhibit multiple weak bands in the region 3100–3000 cm^{-1} due to C-H stretching vibration [14]. In the title molecule, the

very strong intensity band observed at 3065 cm^{-1} in (FT-IR) and very weak intensity bands have assigned at 3069 cm^{-1} in (Raman) C-H ring stretching vibrations. The calculated wave numbers are at 3079 cm^{-1} at CAM-B3LYP method with 6-31G(d,p) and 3210 cm^{-1} at HF method with 6-31G(d,p) basis set respectively. The theoretically calculated C-H vibrations by CAM-B3LYP method of scaled values are good agreement with experimental data as given Table 2.

N-H VIBRATIONS

The title molecule is a type K2DCPAPA, which is, comprises of nitro and amide groups. It has been observed that the presence of N-H in various molecules may be correlated with a constant occurrence of absorption band whose positions are slightly altered from one compound to another this is because of atomic group, which vibrates independently from the other groups in the molecule and has its own frequency. In the all heterocyclic compounds the N-H stretching vibration occur in the region 3600–3300 cm^{-1} [15,16]. The position of absorption in this region depends upon the degree of hydrogen bonding and physical state of the sample. In the present investigation the N-H stretching vibrations have been found very strong band in at 3634 cm^{-1} (FT-IR) assigned to N-H stretching. The calculated wave numbers are at 3301 cm^{-1} by CAM-B3LYP method and 3731 cm^{-1} by HF method at 6-31G (d,p) respectively as given in Table 2.

C=C VIBRATIONS

Generally C=C stretching vibrations in aromatic compounds form a band in the region of 1430–1650 cm^{-1} [17,18]. Accordingly in the present study the C=C stretching vibration of K2DCPAPAareobserved very strong band at 1504 cm^{-1} in FT-IR spectrum. The theoretically computed frequencies at 1511 cm^{-1} at CAM-B3LYP method with 6-31G(d,p) and1611 cm^{-1} at HF method with 6-31G(d,p), respectively. These assignments are in line with the literature.

UV–VISIBLE SPECTRAL ANALYSIS

On the basis of fully optimized ground-state structure, TD-DFT/CAM-B3LYP/6-31G (d,p) calculations have been performed to determine the low-lying excited states of K2DCPAPA. The calculated result involving the vertical excitation energies, oscillator strength (f) and wavelength are carried out and compared with measured experimental wavelength also listed in Table 3. The energy gap between HOMO and LUMO is a critical parameter in determining molecular electrical transport properties [19]. Typically, according to Frank–Condon principle, the maximum absorption peak (max) corresponds in an UV–visible spectrum to vertical excitation. In the calculated value of UV–visible spectrum of K2DCPAPA, there are three absorption bands with a maximum of 280.1 nm. The strong absorption b and at 280.1 nm and the other two calculated values of moderately intense bands. In experimental value [20] of 276 nm is fairly agrees with calculate value of 280.1 nm. The HOMO–LUMO energy gap of K2DCPAPA was calculated at the CAM-B3LYP/6-31G(d,p) level and their values shown below reveals that the energy gap reflect the chemical activity of the molecule. The HOMO is located over all the groups; except the potassium is not involved. However, in LUMO only potassium is occupied the other atoms has not occupied. The atomic orbital compositions of the frontier molecular orbitals are sketched in HOMO–LUMO diagram of Figure 6.

THERMODYNAMIC PROPERTIES

The calculated values of some thermodynamic parameters such as zero point vibrational energy (ZPVE), thermal energy, specific heat capacity, rotational constants, rotational temperature and entropy are listed in Table 4. The electronic energy levels are generally very widely separated in energy compared to the thermal energy kT at room temperature. In

each electronic level, there are several vibrational levels and for each vibrational level, there are several rotational states. This is a simplified and useful model to start with. The total energy is a sum of all these energies and is given by

$$E_{total} = E_{el} + E_{vib} + E_{rot} + E_{trans} + E_{others}$$

The term E_{others} includes nuclear spin energy levels and may also be used later to include the interactions between the first four. Assuming the first three to be independent and neglecting the last term, the molecular partition function (ie, a sum over the molecular energy states) is given by

$$q = \sum e^{-(E_{ele} + E_{vib} + E_{rot} + E_{trans})/kT} = \sum_{el} e^{-\beta E_{el}} \sum_{vib} e^{-\beta E_{vib}} \sum_{rot} e^{-\beta E_{rot}} \sum_{trans} e^{-\beta E_{trans}}$$

Here, the summation is over the electronic, vibrational and rotational states can be done separately since they are assumed to be independent. Therefore,

$$q = q_{el}\, q_{vib}\, q_{rot}\, q_{trans}$$

The molecular partition q function is written as the product of electronic, vibrational, rotational and partition functions. The partition function is a sum over states (of course with the Boltzmann factor β multiplying the energy in the exponent) and is a number. Larger the value of q, larger the number of states which are available for the molecular system to occupy. Since $E_{el}>E_{vib}>E_{rot}>E_{trans}$, there are far too many translational states available compared to the rotational, vibrational and electronic states. q_{el} is very nearly unity, q_{vib} and q_{rot} are in the range of 1 to 100 while q_{trans} can be much in excess of 10^{20}. We shall calculate the values of these qs and indicate how these qs are useful in calculating the equilibrium constants. The biggest value of zero point energy of K2DCPAPA is 142.26475 kcal/mol obtained at HF/cc-pVDZ whereas the smallest value is 134.33462 kcal/mol obtained at CAM-B3LYP/cc-pVDZ. The dipole moment of the molecule was also calculated by two methods with basis set. Dipole moment reflects the molecular charge distribution and is given as a vector in three dimensions. Therefore, it can be used as descriptor to depict the charge movement across the molecule depending upon the centers of positive and negative charges. For charged systems, dipole moment value depends on the choice of origin and molecular orientation. As a result of ab initio method is the highest dipole moments were observed for HF/6-31G(p,d) whereas the smallest one was observed for CAM-B3LYP/6-31G(p,d) in K2DCPAPA.

ELECTROSTATIC POTENTIAL

Molecular electrostatic potential (MESP) at a point in the space around a molecule gives an indication of the net electrostatic effect produced at that point by the total charge distribution (electron +nuclei) of the molecule and correlates with dipole moments, electro negativity, partial charges and chemical reactivity of the molecule. It provides a visual method to understand the relative polarity of the molecule. An electron density is surface mapped with electrostatic potential surface depicts the size, shape, charge density and reactive sites of the molecules.

The different values of the electrostatic potential represented by different colors; red represents the regions of the most negative electrostatic potential, blue represents the regions of the most positive electrostatic potential and green represents the region of zero potential. Potential increases in the order red <orange<yellow <green<blue. Such mapped electrostatic potential surfaces have been plotted of title molecule in CAM-B3LYP/6-31 basis set using the computer software Gauss view. Projections of these surfaces along the molecular plane and a perpendicular plane are given in Figure 7. This figure provides a visual representation of the chemically active sites and comparative reactivity of atoms.

^{13}Cand ^{1}H NMR Chemical Shift

The ^{13}C and ^{1}H NMR spectrum theoretically with the aid of Gaussian and facio software program is shown in Figures 8 and 9. Table 5 present the predicted chemical shift values of K2DCPAPA obtained by the DFT, HF and ChemDraw Ultra 8.0 software package along with the shielding values. In general, highly shielded electrons appear at downfield (lower chemical shift) and vice versa. The predicted chemical shift values by the ChemDraw Ultra software program are in fairly agreement with theoretical values. The carbon atom C_8 appearing at very higher chemical shift value (178.48 ppm) due to double bond of oxygen atom and hence the shielding is very small and appears up field (see Table 5). In DFT-calculated atomic charges revealed that the more electron-rich atoms are C_9, C_{19}, and C_{20} they are highly shielded atoms and appear at downfield (lower chemical shift). In this study, a good correlation between atomic charges and chemical shift was made.

Table 5 gives the ^{1}H NMR predicted chemical shift values obtained by the DFT, HF methods, experimental and Chem Draw Ultra 10.0 software. The predicted shielding values for each atom in the K2DCPAPA molecule by CAM-B3LYP is given in Table 5. The predicted chemical shift values by the DFT theoretical methods fairly agrees from the ChemDraw Ultra values. There is no higher absolute shielding for our compound. DFT, HF methods predict that all the hydrogen atoms (H_{21} to H_{30}) absolute shielding values is almost 8.0 expect H_{25}, H_{26}, H_{27}. In Chemical shift values, the Chem Draw Ultra are fairly agrees with theoretical values.

MULLIKEN POPULATION ANALYSIS

Mulliken atomic charge analysis plays an important role in the application of theoretical calculation to molecular system, as atomic charges affect properties of molecular systems [21]. The electronic charge on an atom determines the bonding capability and molecular conformation. The atomic charge values were obtained by the Mulliken population analysis [22]. Mulliken population analysis was performed on the title molecule by CAM-B3LYP and HF method using 6-31G(d,p) as the basis set and presented in Table 6. The oxygen atoms O10 and O11 have charges -0.9621, and -0.8941e respectively in CAM-B3LYP method. Of which O10 has the highest negative value. C8 has the maximum positive charge of 1.0671e and K1 has the next maximum charge of 0.8488e. Hence, the oxygen atoms attract the carbon atom C8 and the potassium atom K1. N12 atom has negative charge of -0.8956e and the H27 atom attached to it has positive charge 0.3482e in CAM-B3LYP method. Majority of hydrogen atoms exhibit positive charge in CAM-B3LYP method. The net charge of hydrogen atoms was 0.5687e in CAM-B3LYP. The presence of negative charge on nitrogen and oxygen atoms and net positive charge on hydrogen atoms may suggest the formation of in tramolecular interaction in solid forms [23]. The advantage of this population analysis is that it is useful for comparing changes in partial charge assignment between two different geometries with the same size basis set. The mulliken charges obtained by CAM-B3LYP/6-31G(d,p) and HF/6-31G(d,p) methods are shown in Figure 10.

NATURAL BOND ORBITAL ANALYSIS

Natural Bond Analysis (NBO) stresses the role of intermolecular orbital interaction in the complex, particularly charge transfer. This is carried out by considering all possible interactions between filled donor and empty acceptor natural bond orbital and estimating their energetic importance by second order perturbation theory. The NBO analysis of K2DCPAPA has provided detailed insight into the nature of electronic conjugation between the bonds in this molecule. Natural bond analysis is a measure of delocalization or hyper conjugation. The hyper conjugation interaction energy was

deduced from the second order perturbation approach [50].

$$E^{(2)} = \Delta E_{ij} = q_i \frac{F(i,j)^2}{\epsilon j - \epsilon i}$$

Where q_i is the donor orbital occupancy, Єi and $Є_j$ are diagonal elements and F (i,j) is the off diagonal NBO Fock matrix element. The larger the $E^{(2)}$ value, the more intensive is the interaction between electron donors and electron acceptors. The more the donating tendency of electron donors to electron acceptors, then greater will be the extent of conjugation of the whole system [24].

The interaction between lone pair LP (2) of type O10 with σ* (C8 – O11) results in a stabilization energy of 23.02 KJ/mol and lone pair LP (2) of type O11 with σ* (C8 – O10) results in stabilization energy of 23.02 KJ/mol. These indicate larger delocalization. The intermolecular hype conjugative interaction of σ (C8 – O11) to σ* (C8 - O11) leading to strong stabilization of 2.68 KJ/mol. The intermolecular hyper conjugative interaction of σ (C2 – C9) to σ* (C8 – O11) and σ (C6 – C7) to σ* (C2 –C7) leads to stabilization of 3.72 and 3.73 KJ/mol respectively. These interactions are observed as increase in electron density in ant bonding orbital that weakens the respective bonds. These charge transfer interactions in K2DCPAPA are responsible for chemical properties. Hence, K2DCPAPA structure is stabilized by these orbitals interactions. In K2DCPAPA, the oxygen has larger percentage of NBO and gives the larger polarization co-efficient because it has the higher electro negativity. The calculated values of $E^{(2)}$ are given in Table 7.

FIRST ORDER HYPERPOLARIZABILITY

The First order Hyperpolarizability (β) is a measure of induced dipole in a molecule in the presence of an electric field. The large value of hyperpolarizability is a measure of the non-linear optical activity of the molecular system and is associated with the intermolecular charge transfer resulting from the electron cloud movement through Π conjugated frame work from electron donor to electron acceptor groups. Non-linear optical (NLO) responses induced in various materials are of great interest in recent years because of the potential applications in photonic technologies such as optical communication, computing data storage and image processing [25]. Recent efforts have been focused to develop organic molecules with large molecular non-linear optical response, improved optical transparency and good thermal stability [26]. The first order hyperpolarizability is a third rank tensor described by 3 X 3 X 3 matrix. The 27 components of the 3D matrix can be reduced to 10 components due to the Klein man symmetry [27]. The components of β are defined as the coefficients in the taylor series expansion of the energy in the external electric field. The expression of the external Electric field when it becomes weak and homogeneous is

$$E = E^0 - \mu_\alpha F_\alpha - \frac{1}{2\alpha_{\alpha\beta}F_\alpha F_\beta} + \frac{1}{6\beta_{\alpha\beta\gamma}F_\alpha F_\beta F_\gamma}$$

E^0 is the energy of the unperturbed molecules, F_α is the field at the orgin, μ_α, $\alpha_{\alpha\beta}$& $\beta_{\alpha\beta\Upsilon}$ are the components of dipole moment, polarizability and the first order hyperpolarizability respectively. The total static dipole moment μ, the mean polarizability α_0, the anisotropy of the polarizability Δα and mean first order hyperpolarizability β_0 using the x,y and z components are defined as follows.

$$\mu = [\mu_x^2 + \mu_y^2 + \mu_z^2]^{1/2}$$

$$\alpha_0 = \frac{[\alpha_{xx} + \alpha_{yy} + \alpha_{zz}]}{3}$$

$$\Delta\alpha = 2^{-1/2}[(\alpha_{xx} - \alpha_{yy})^2 + (\alpha_{yy} - \alpha_{zz})^2 + (\alpha_{zz} - \alpha_{xx})^2]^{1/2}$$

$$\beta_0 = (\beta_x^2 + \beta_y^2 + \beta_z^2)^{1/2} \text{and}$$

$$\beta_x = \beta_{xxx} + \beta_{xyy} + \beta_{xzz}$$

$$\beta_y = \beta_{yyy} + \beta_{xxy} + \beta_{yzz}$$

$$\beta_z = \beta_{zzz} + \beta_{xxz} + \beta_{yyz}$$

Since the values of the polarizabilities (α) and hyperpolarizability (β) are reported in atomic units (a.u.), the calculated values were converted into electrostatic units (esu). [α: 1a.u. = 0.1482 X10^{-24}esu; β: 1a.u. = 8.639 X 10^{-33}esu]. The first order hyperpolarizability(β) of the molecule along with related properties were calculated using HF/6-31G(d,p) and CAM-B3LYP/6-31G(d,p) methods are presented in Table 8. Urea is one of the molecules which has good non-linear optical property and it is has been used as a critical parameter for comparative studies. (μ = 1.3732 debye and β = 0.3728 X 10^{-30}esu). The highest value of dipole moment is observed for component μ_x. In this direction, this value is equal to 0.84 Debye and the lowest value of the dipole moment of the 2DCPAPAA compound is lx component (-2.53). In HF method, dipole moment (μ) was nearly 2.0 times greater than urea and the hyperpolarizability was 1.2 times greater than urea. In B3LYP method, the dipole moment was 2.1 times greater than urea and hyperpolarizability was 1.4 times greater than urea. Hence the title compound has good non-linear property.

CHEMICAL REACTIVITY

Global Reactivity Descriptors

Conceptual density functional theory based global reactivity descriptors are used to understand the relationship between structures, stability and global chemical reactivity. These descriptors are employed in the development of quantitative structure activity (QSAR), structure property (QSPR) and structure toxicity (QSTR) relationships [28]. QSAR methodology is one of the most powerful tools for describing the relationships between biological activity and the physicochemical characteristics of molecules.

The global descriptor of hardness has been an indicator of overall stability of the system. According to the Koop man's theorem [29] associated within the framework of HF self-consistent field molecular orbital theory the ionization energy and electron affinity can be expressed through HOMO and LUMO orbital energies.

$$I = -E_{HOMO} \text{ and } A = -E_{LUMO}$$

The higher HOMO energy corresponds to the more reactive molecule in the reactions with electrophiles, while lower LUMO energy is essential for molecular reactions with nucleophiles [30]. Knowing the HOMO-LUMO energy gap, the nature of the molecule (hard or soft) can be determined. The molecule having a large energy gap are known as hard molecules [31] and those with less energy gap are known as soft molecules. The soft molecules are more polarizable than the hard ones as they require less energy for excitation. The hardness of the molecule is determined by the formula

$$\eta = \frac{1}{2}(I - A)$$

$$\eta = \frac{1}{2}(E_{LUMO} - E_{HOMO})$$

and global softness inverse of global hardness is obtained by the formula

$$S = \frac{1}{2\eta}$$

The electron affinity can also be used in combination with ionization energy to give electronic chemical potential (μ) defined by Parr and Pearson [32] as the characteristic of electro negativity of molecules.

$$\mu = -\frac{1}{2}(I + A)$$

$$\mu = \frac{1}{2}\ (E_{LUMO} + E_{HOMO})$$

$$\mu = -\chi$$

$$\chi = -\frac{1}{2}(E_{LUMO} + E_{HOMO})$$

The global electrophilicity index (ω) was introduced by Parr [60] and calculated using the electronic potential μ and chemical hardness η

$$\omega = \frac{\mu^2}{2\eta}$$

According to this definition, index measures the propensity of a species to accept electrons. A good, more reactive, nucleophile is characterized by a lower value of μ, ω and conversely a good electrophile is characterized by a high value of μ and ω. Table 9 presents the values of electro negativity (χ), chemical potential (μ), global hardness (η), global softness (S) and global electrophilicity index (ω).

CONCLUSIONS

The molecular geometry of the molecule in the ground state has been calculated by using RHF and DFT (CAM-B3LYP) methods with 6-31G (d,p) basis set. Several thermodynamical parameters were obtained and analyzed with RHF and DFT methods using the same basis set. The HOMO-LUMO energy gap helped in analyzing the chemical reactivity of the molecule. Mulliken charges of the molecule were studied by both the RHF and DFT methods. The 1H and 13C NMR chemical shifts were calculated and compared with the Chemsoft values. The calculated dipole moment and first order hyperpolarizability results indicate that the molecule has a reasonably good nonlinear optical behavior. The NBO analysis indicated the intramolecular charge transfer between the bonding and antibonding orbitals. MESP confirmed the presence of different negative and positive potential sites of the molecule in accordance with the total electron density surface. On comparing the results, CAM-B3LYP method was more accurate, proving that DFT is a reliable method for molecular structural studies.

REFERENCES

1. *Altman R, Bosch B, Brune K, Patrignani P, Young C (2015). "Advances in NSAID development: evolution of diclofenac products using pharmaceutical technology". Drugs. 75: 859–77.*
2. *"RUFENAL". Birzeit Pharmaceutical Company. Archived from the original on 2011-05-26. 3*
3. *Frisch M J, Trucks G W, Schlegel H B, Scuseria G E, Robb M A, Cheese man J R, Scalmani G, Barone V, Mennucci B, Petersson G A, Nakatsuji H, Caricato M, Li X, Hratchian H P, Izmaylov A F, Bloino J, Zheng G, Sonnenberg J L, Hada M, Ehara M, Toyota K, Fukuda R, Hasegawa J, Ishida M, Nakajima T, Honda Y, Kitao O, Nakai H, Vreven T, Montgomery J A*

Jr, Peralta J E, Ogliaro F, Bearpark M, Heyd J J, Brothers E, Kudin K N, Staroverov V N, Kobayashi R, Normand J, Raghavachari K, Rendell A, Burant J C, Iyengar S S, Tomasi J, Cossi M, Rega N, Millam J M, Klene M, Knox J E, Cross J B, Bakken V, Adamo C, Jaramillo J, Gomperts R, Stratmann R E, Yazyev O, Austin A J, Cammi R, Pomelli C, Ochterski J W, Martin R L, Morokuma K, Zakrzewski V G, Voth G A, Salvador P, Dannenberg J J, Dapprich S, Daniels A D, Farkas O, Foresman J B, Ortiz J V, Cioslowski J, Fox DJ. GAUSSIAN 09W. Wallingford, CT: Gaussian, Inc.; 2009.

4. *Becke A D, Density-functional thermo chemistry. 2. The effect of the Perdew–Wang generalized-gradient correlation correction. J Chem Phys. 1992; 97: 9173–9177.*
5. *Becke A D, Density-functional thermo chemistry. III. The role of exact exchange, Chem Phys. 1993; 98:5648–5652.*
6. *Lee C, Yang W, Parr R G. Development of the Colle–Salvetticongelation energy formula into a functional of the electron density. Phys Rev B. 1988; 37:785–789.*
7. *Yanai T, Tew D P, Handy N C. A new hybrid exchange-correlation functional using the Coulomb-attenuating method (CAM-B3LYP). Chem Phys Lett. 2004; 393:51–57.*
8. *Handy N C, Murray C W, Amos R D. Study of CH4, C2H2, C2H4and C6H6 using Kohn–Sham theory. J Phys Chem. 1993; 97:4392–4396.*
9. *Handy N C, Maslen P E, Amos R D, Andrews J S, Murray C W, Laming G J. The harmonic frequencies of benzene. Chem Phys Lett. 1992; 197:506–515.*
10. *Stephens P J, Devlin F J, Chabalowski C F, Frisch M J. Ab initio calculation of vibrational absorption and circular dichroism spectra using density functional force fields: a comparison of local, nonlocal, and hybrid density functionals. J Phys Chem. 1995; 99:16883–16902.*
11. *Sutton LE. Tables of interatomic distances and configuration in molecules and ions. WI: Chemical Society, Burlington House; 1958. p. 18*
12. *Socrates G. Infrared and Raman characteristic frequencies. 3rd ed. ChiK2DCPAPAter: Wiley; 2001.*
13. *Prasad R L, Kushwaha A, Kumar M, Yadav R A. Infrared and ab initio studies of conducting molecules: 2,5-diamino-3,6-dichloro-1,4-benzoquinone. Spectrochim Acta A. 2008; 69:304–311.*
14. *Udhayakala P, Rajendiran T. V, Seshadri S, Gunasekaran S, J. Chem. Pharm. Res. 3 (3) (2011) 610–625.*
15. *Gunasekaran S, Kumaresan K, ArunBalaji R, Anand G, SeshadriS, Pramana. 71(6) (2008) 1291–1300.*
16. *Wang Y, Saebo S, Pittman C.U, J. Mol. Struct. 281 (1993) 91–288.*
17. *Gunasekaran S, Anitha B, Seshadri S, Indian J. Pure Appl. Phys. 48 (2010) 183–191.*
18. *Varsanyi G, Assignments for vibrational Spectra of seven Hundred Benzene Derivatives, AdomHilger, 1974.*
19. *Silverstein R M, Bassler G C, Morrill T C, Spectrometric Identification of Organic Compounds, 5th ed., John Wiley & Sons, Inc., New York, 1981*
20. *Govindasamy P, Gunasekaran S, Spectroscopic (FT-IR, FT-Raman and UV) investigation, NLO, NBO, molecular orbital and MESP analysis of 2-{2-[(2,6-dichlorophenyl)amino]phenyl}acetic acid, SpectrochimicaActa Part A: Molecular and Biomolecular Spectroscopy 136 (2015) 1543–1556*
21. *Rastogi V K, Palatox M A, Mittal L, Peica N, Kiefer W, Lang K, Ohja P, J. Raman Spectrosc. 38 (2007) 1227-1241.*
22. *Mulliken R S, J.Chem. Phys. 23 (1955) 1833-1840.*

23. *L. Xiao –Hong etal, Theor. Chem. 969 (2011) 27-34.*
24. *Cheol Ho Choi, Miklos Kertesz, J. Phys. Chem. A 101 (1997) 3823- 3831.*
25. *Parasad P N, Williams D J, Introduction to Nonlinear Optical Effects in Molecular and Polymers; John Wiley & Sons: New York, 1991.*
26. *Gyoosoon Park, Woo Sik Jung, Choon Sup Ra, Bull. Korean Chem. Soc. 25(9) (2004) 1427-1429.*
27. *Kleinman D A, Phys. Rev. 126 (1962) 1977-1979.*
28. *Vijayaraj R, Subramanian V, Chattaraj P K, J. Chem. Theo. Comput. 5(10) (2009) 2744-2753.*
29. *Koopmans T, Physica 1 (1933) 104-113.*
30. *Rauk A, Orbital Interaction Theory of Organic Chemistry, 2nd Ed., John Wiley & Sons, New York, 2001.*
31. *Pearson R G, J. Am. Chem. Soc. 107 (1985) 6801-6806.*
32. *Parr R G, Pearson R G, J. Am. Chem Soc. 105, (1983) 7512-7516.*

APPENDICES

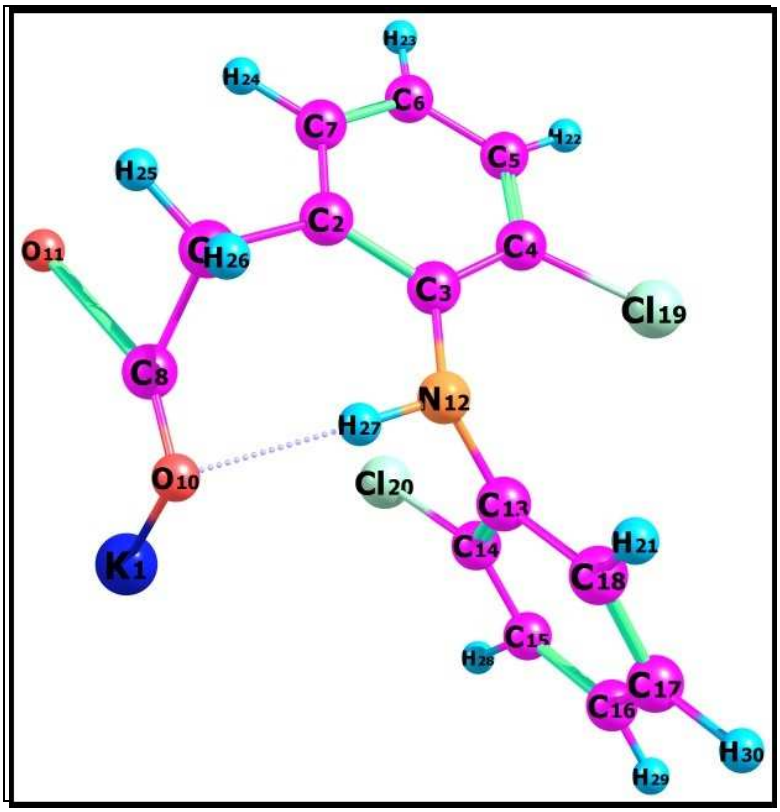

Figure 1: Optimized Molecular Structure and Atomic Numbering of K2DCPAPA

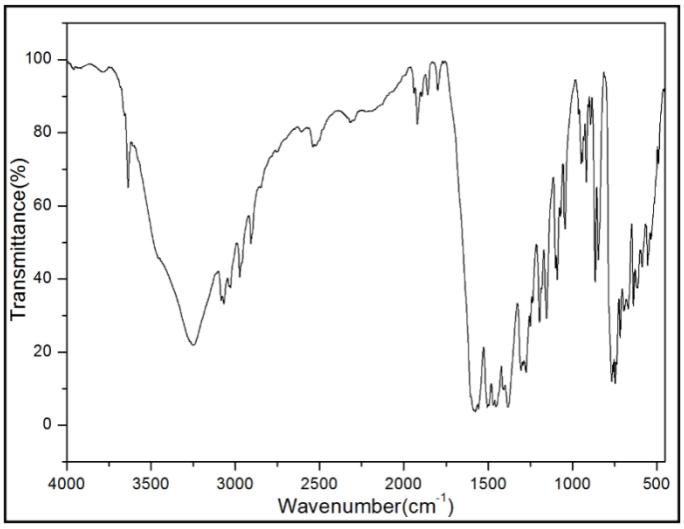

Figure 2: FT-IR Spectrum forK2DCPAPA

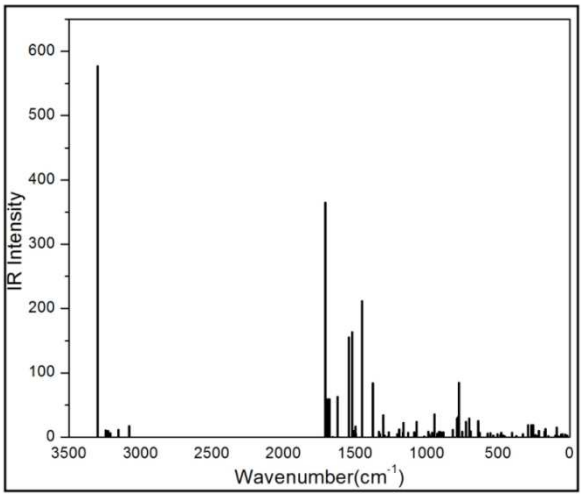

Figure 3: Stimulated Vibrational Spectrum of K2DCPAPA

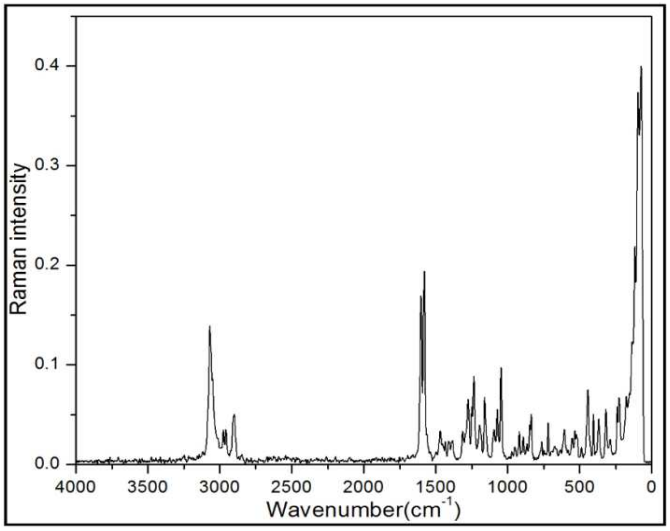

Figure 4: FT-Raman Spectrum for K2DCPAPA

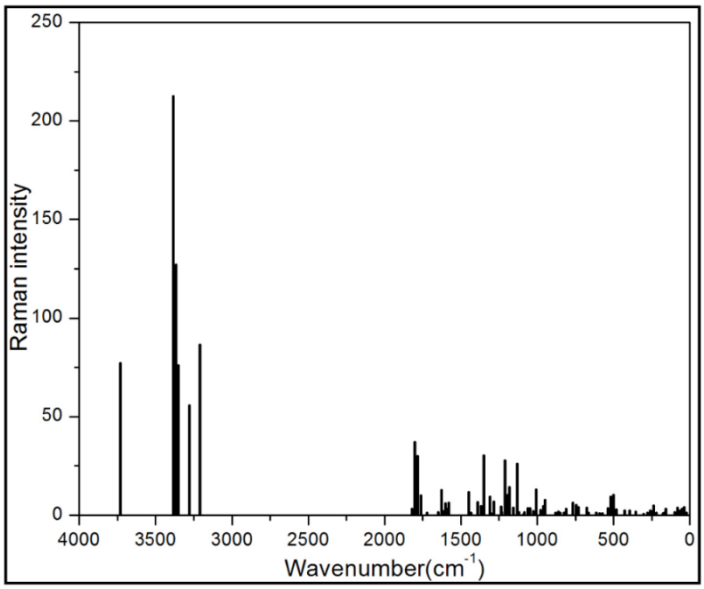

Figure 5: Stimulated Vibrational Spectrum of K2DCPAPA

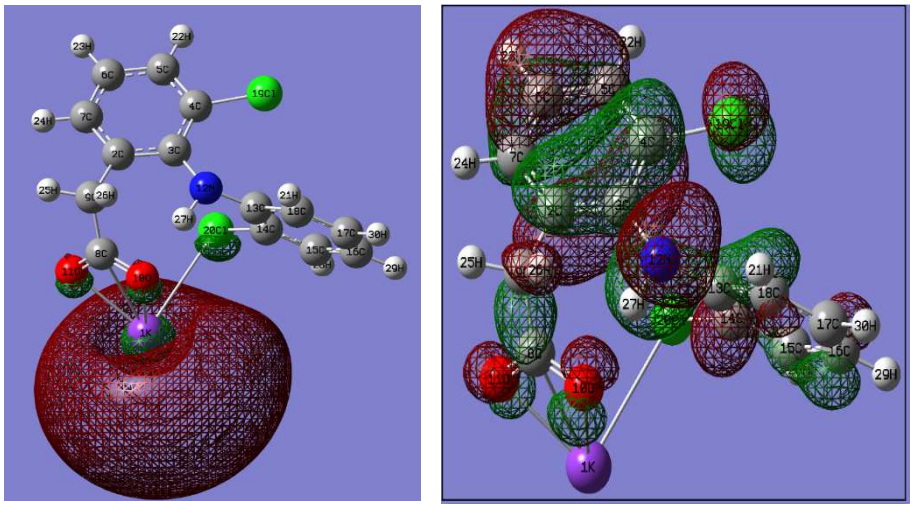

LUMO (First Excited State) **HOMO (Ground State)**

Figure 6: The Atomic Orbital Composition of the Frontier Molecular Orbital for K2DCPAPA

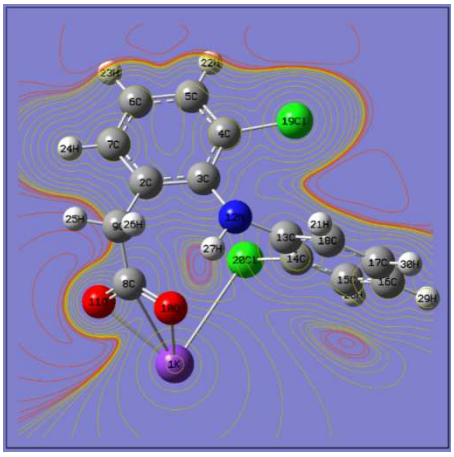

Figure 7: The Contour Map of Electrostatic Potential of K2DCPAPA

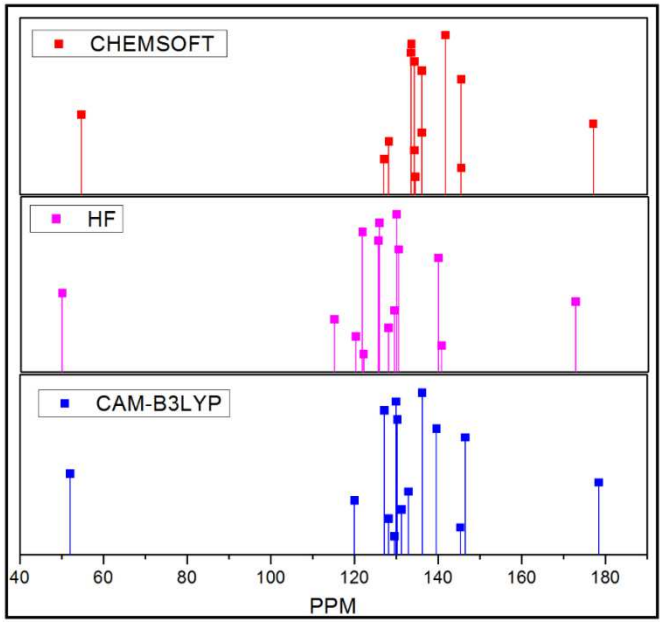

Figure 8: ^{13}C NMR Spectrum of K2DCPAPA

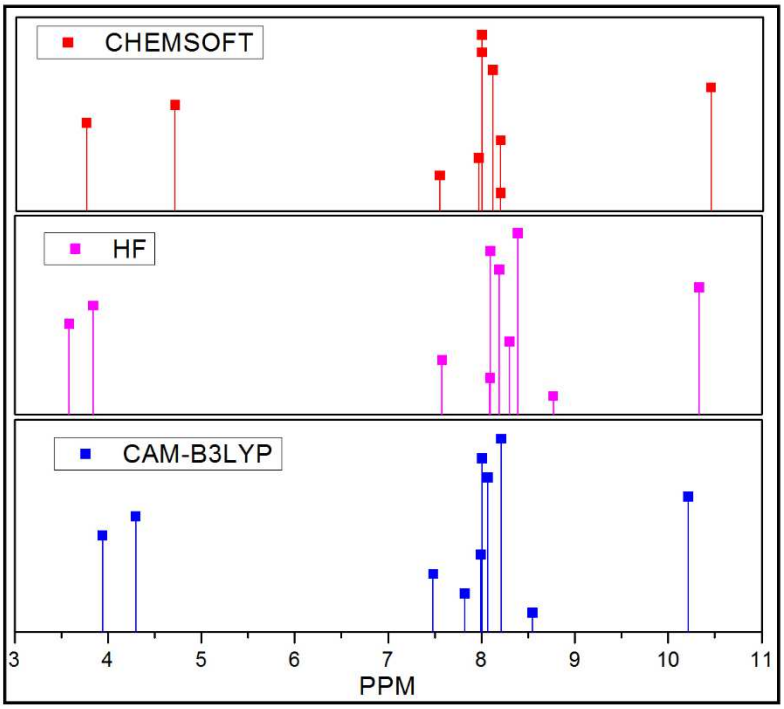

Figure 9: ^{1}H NMR Spectrum of K2DCPAPA

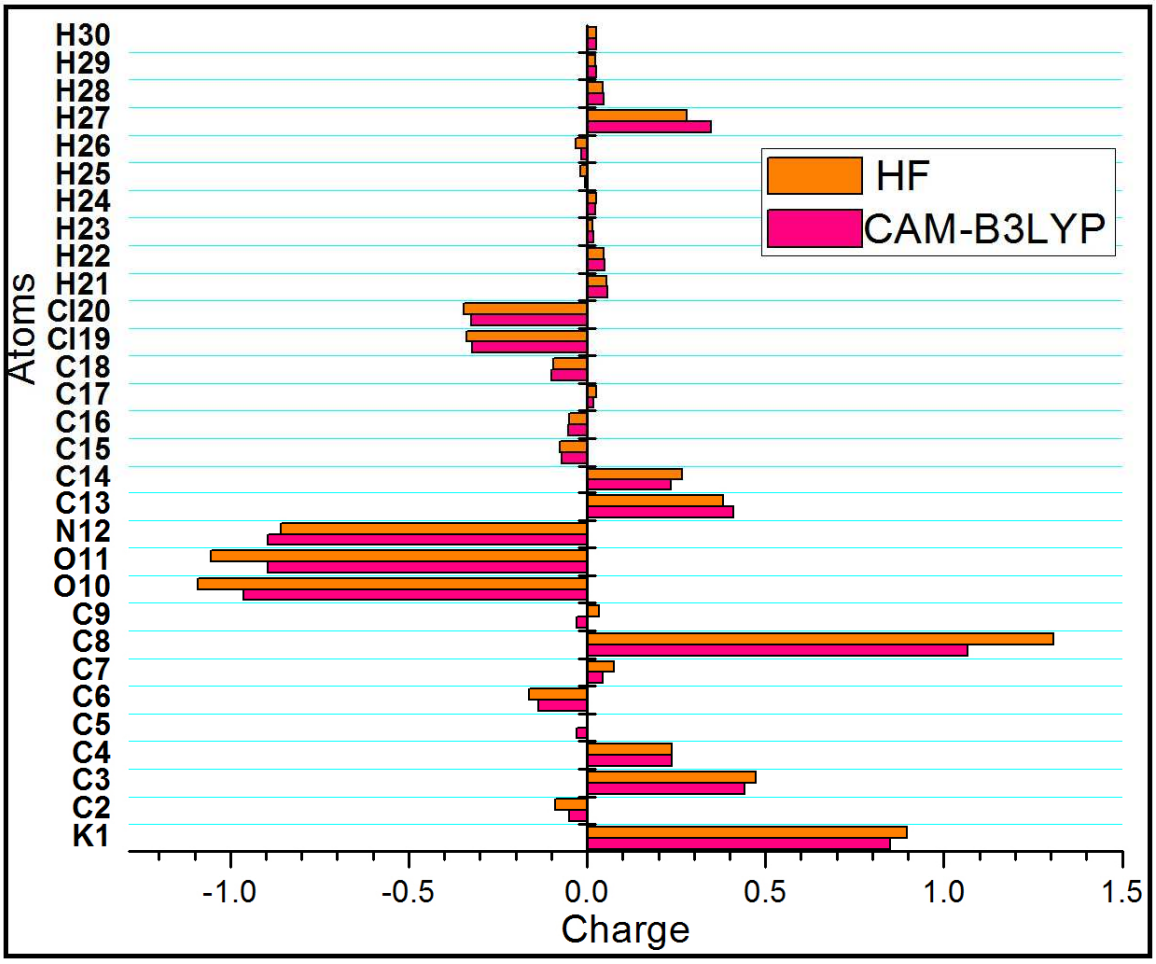

Figure 10: Plot of Mulliken Charges of K2DCPAPA

Table 1: Geometrical Parameters of K2DCPAPA Obtained by CAM-B3LYP and HF Methods

Structural Parameter	CAM-B3LYP	HF	Ref	Structural Parameter	CAM-B3LYP	HF	Ref
Bond Length (A°)				**Dihedral Angle (°)**			
C(8)-K(1)	2.819	2.867		Cl(20)-K(1)-C(8)-C(9)	7.7	7.9	-
O(10)-K(1)	2.538	2.569		C(8)-K(1)-Cl(20)-C(14)	83.3	81.5	-
O(11)-K(1)	2.537	2.570		O(10)-K(1)-Cl(20)-C(14)	56.2	54.9	-
Cl(20)-K(1)	3.261	3.444	3.104	O(11)-K(1)-Cl(20)-C(14)	107.9	105.8	-
C(3)-C(2)	1.418	1.414	1.395	C(4)-C(3)-C(2)-C(7)	4.0	4.4	4.0
C(7)-C(2)	1.389	1.382	1.395	N(12)-C(3)-C(2)-C(7)	-179.8	-179.6	-180.0
C(9)-C(2)	1.517	1.523	1.497	C(4)-C(3)-C(2)-C(9)	-173.9	-173.0	-174.0
C(4)-C(3)	1.403	1.394	1.395	N(12)-C(3)-C(2)-C(9)	1.9	3.0	0.0
N(12)-C(3)	1.396	1.399	1.266	C(6)-C(7)-C(2)-C(3)	-0.9	-1.1	0.0
C(5)-C(4)	1.389	1.386	1.395	H(24)-C(7)-C(2)-C(3)	179.2	179.0	180.0
Cl(19)-C(4)	1.755	1.752	1.711	C(6)-C(7)-C(2)-C(9)	177.0	176.4	180.0
C(6)-C(5)	1.383	1.375	1.395	H(24)-C(7)-C(2)-C(9)	-2.8	-3.5	0.0
H(22)-C(5)	1.084	1.074	1.100	C(8)-C(9)-C(2)-C(3)	-65.2	-69.4	-66.1
C(7)-C(6)	1.389	1.386	1.395	H(25)-C(9)-C(2)-C(3)	174.6	170.7	174.9
H(23)-C(6)	1.084	1.075	1.100	H(26)-C(9)-C(2)-C(3)	56.2	52.8	56.1
H(24)-C(7)	1.085	1.075	1.100	C(8)-C(9)-C(2)-C(7)	116.9	113.2	116.9
C(9)-C(8)	1.534	1.531	1.509	H(25)-C(9)-C(2)-C(7)	-3.3	-6.7	-3.1
O(10)-C(8)	1.274	1.251	1.250	H(26)-C(9)-C(2)-C(7)	-121.7	-124.7	-121.9
O(11)-C(8)	1.251	1.235	1.250	C(5)-C(4)-C(3)-C(2)	-4.6	-5.0	0.0

Table 1: Contd.,							
H(25)-C(9)	1.091	1.081	1.113	Cl(19)-C(4)-C(3)-C(2)	173.6	173.2	174.0
H(26)-C(9)	1.095	1.086	1.113	C(5)-C(4)-C(3)-N(12)	179.9	179.3	180.0
O(10)-H(27)	1.809	1.989	-	Cl(19)-C(4)-C(3)-N(12)	-2.0	-2.6	0.0
C(13)-N(12)	1.417	1.419	1.266	C(13)-N(12)-C(3)-C(2)	146.7	144.7	146.7
H(27)-N(12)	1.028	1.002	1.050	H(27)-N(12)-C(3)-C(2)	8.7	7.1	8.0
C(14)-C(13)	1.400	1.391	1.395	C(13)-N(12)-C(3)-C(4)	-37.7	-39.6	-36.7
C(18)-C(13)	1.397	1.392	1.395	H(27)-N(12)-C(3)-C(4)	-175.7	-177.3	-176.0
C(15)-C(14)	1.389	1.386	1.395	C(6)-C(5)-C(4)-C(3)	1.9	2.1	0.0
Cl(20)-C(14)	1.760	1.754	1.719	H(22)-C(5)-C(4)-C(3)	-179.0	-178.8	-180.0
C(16)-C(15)	1.387	1.381	1.395	C(4)-Cl(19)-C(5)-C(6)	-176.3	-176.2	-176.0
H(28)-C(15)	1.084	1.074	1.100	C(4)-Cl(19)-C(5)-H(22)	2.8	3.0	2.0
C(17)-C(16)	1.390	1.386	1.395	C(7)-C(6)-C(5)-C(4)	1.3	1.5	0.0
H(29)-C(16)	1.085	1.075	1.100	H(23)-C(6)-C(5)-C(4)	-179.9	-180.0	-180.0
C(18)-C(17)	1.386	1.380	1.395	C(7)-C(6)-C(5)-H(22)	-177.8	-177.7	-180.0
H(30)-C(17)	1.085	1.075	1.100	H(23)-C(6)-C(5)-H(22)	0.8	0.9	0.0
H(21)-C(18)	1.084	1.074	-	C(2)-C(7)-C(6)-C(5)	-1.8	-1.9	0.0
				H(24)-C(7)-C(6)-C(5)	178.0	178.0	180.0
Bond angle (°)				H(23)-C(6)-C(7)-C(2)	179.6	179.5	-
C(7)-C(2)-C(3)	119.7	119.6	120.0	H(24)-C(7)-C(6)-H(23)	-0.6	-0.6	0.0
C(9)-C(2)-C(3)	121.4	121.7	120.0	C(2)-C(9)-C(8)-O(10)	90.8	94.7	90.0
C(9)-C(2)-C(7)	118.9	118.6	120.0	H(25)-C(9)-C(8)-O(10)	-148.9	-145.3	-149.0
C(4)-C(3)-C(2)	117.2	117.3	120.0	H(26)-C(9)-C(8)-O(10)	-31.6	-28.2	-32.0
N(12)-C(3)-C(2)	118.8	118.5	120.0	C(2)-C(9)-C(8)-O(11)	-85.6	-82.8	-86.0
C(4)-C(3)-N(12)	123.9	124.0	120.0	H(25)-C(9)-C(8)-O(11)	34.8	37.2	34.0
C(3)-C(4)-C(5)	122.2	122.0	120.0	H(26)-C(9)-C(8)-O(11)	152.1	154.3	152.0
C(3)-C(4)-Cl(19)	121.2	121.8	120.7	C(14)-C(13)-N(12)-C(3)	-51.7	-54.3	-51.0
Cl(19)-C(4)-C(5)	116.6	116.1	115.3	C(18)-C(13)-N(12)-C(3)	134.0	130.8	134.0
C(6)-C(5)-C(4)	120.0	120.1	120.0	C(14)-C(13)-N(12)-H(27)	87.8	84.7	87.0
H(22)-C(5)-C(4)	118.8	118.8	120.0	C(18)-C(13)-N(12)-H(27)	-86.5	-90.2	-87.0
H(22)-C(5)-C(6)	121.3	121.1	120.0	C(15)-C(14)-C(13)-N(12)	-177.3	-177.2	-180.0
C(7)-C(6)-C(5)	118.9	118.8	120.0	Cl(20)-C(14)-C(13)-N(12)	2.3	2.8	0.0
H(23)-C(6)-C(5)	120.4	120.5	120.0	C(15)-C(14)-C(13)-C(18)	-2.9	-2.3	0.0
H(23)-C(6)-C(7)	120.7	120.7	120.0	Cl(20)-C(14)-C(13)-C(18)	176.6	177.7	178.0
C(2)-C(7)-C(6)	122.0	122.0	120.0	C(17)-C(18)-C(13)-N(12)	176.4	176.5	180.0
H(24)-C(7)-C(2)	118.2	118.5	120.0	H(21)-C(14)-C(13)-C(18)	-179.6	-179.8	-
H(24)-C(7)-C(6)	119.8	119.5	120.0	C(16)-C(15)-C(14)-C(13)	2.2	1.9	0.0
C(9)-C(8)-O(10)	116.3	116.7	120.0	H(28)-C(15)-C(14)-C(13)	-178.2	-178.4	-180.0
C(9)-C(8)-O(11)	118.7	118.1	120.0	C(16)-C(15)-C(14)-Cl(20)	-177.4	-178.2	-180.0
O(10)-C(8)-O(11)	124.9	125.1	124.0	H(28)-C(15)-C(14)-Cl(20)	2.3	1.5	0.0
C(2)-C(9)-C(8)	113.1	113.4	109.5	C(13)-K(1)-C(14)-Cl(20)	-78.1	-78.9	-
C(2)-C(9)-H(25)	108.5	108.2	109.4	C(15)-K(1)-C(14)-Cl(20)	101.4	101.2	-
C(2)-C(9)-H(26)	110.1	110.1	109.5	C(17)-C(16)-C(15)-C(14)	0.0	-0.1	0.0
C(8)-C(9)-H(25)	108.3	108.1	109.4	H(29)-C(16)-C(15)-C(14)	179.9	179.9	180.0
C(8)-C(9)-H(26)	108.3	108.8	109.5	C(17)-C(16)-C(15)-H(28)	-179.7	-179.9	180.0
H(25)-C(9)-H(26)	108.3	108.1	109.5	H(29)-C(16)-C(15)-H(28)	0.3	0.2	0.0
C(13)-N(12)-C(3)	126.0	126.2	120.0	C(18)-C(17)-C(16)-C(15)	-1.3	-1.0	0.0
H(27)-N(12)-C(3)	113.1	112.7	120.0	H(30)-C(17)-C(16)-C(15)	179.7	179.8	180.0
H(27)-N(12)-C(13)	108.8	108.8	110.0	C(18)-C(17)-C(16)-H(29)	178.8	179.0	180.0
N(12)-C(13)-C(14)	125.2	125.4	125.0	H(30)-C(17)-C(16)-H(29)	-0.2	-0.2	0.0
N(12)-C(13)-C(18)	117.8	117.4	118.0	C(13)-C(18)-C(17)-C(16)	0.5	0.5	0.0
C(18)-C(13)-C(14)	116.8	117.0	116.0	H(21)-C(18)-C(17)-C(16)	-178.3	-178.5	-
C(15)-C(14)-C(13)	122.0	121.8	120.0	C(13)-C(18)-C(17)-H(30)	179.5	179.7	180.0
Cl(20)-C(14)-C(13)	120.6	121.2	120.0	H(21)-C(18)-C(17)-H(30)	0.8	0.7	-
Cl(20)-C(14)-C(15)	117.4	117.1	117.0				
C(16)-C(15)-C(14)	119.7	119.9	120.0				

Table 1: Contd.,							
H(28)-C(15)-C(14)	119.4	119.4	120.0				
H(28)-C(15)-C(16)	120.9	120.7	120.0				
C(17)-C(16)-C(15)	119.6	119.5	120.0				
H(29)-C(16)-C(15)	119.7	119.8	120.0				
H(29)-C(16)-C(17)	120.7	120.7	120.0				
C(18)-C(17)-C(16)	120.0	119.9	120.0				
H(30)-C(17)-C(16)	120.2	120.3	120.0				
H(30)-C(17)-C(18)	119.8	119.8	120.0				
C(17)-C(18)-C(13)	121.9	121.9	120.0				
C(21)-C(18)-C(13)	117.0	117.3	-				
C(21)-C(18)-C(17)	121.0	120.8	-				
C(14)-Cl(20)-K(1)	100.5	105.5	101.2				

Table 2: The Observed and Calculated Frequencies of K2DCPAPA using CAM-B3LYP and HF Methods

FT-IR	FT-Raman	CAMB3LYP/ 6-31G(d,p)	IR Intensity	HF/ 6-31G(d,p)	IR Intensity	Vibrational Band Assignment PED(%)
3634		3301	576.59	3731	273.60	γNH (99)
3249		3245	5.55	3387	7.90	γCH (89)
		3243	10.11	3384	15.94	γCH (97)
		3238	8.83	3380	16.76	γCH(99)
		3228	8.11	3368	19.24	γCH(99)
		3228	9.10	3366	17.52	γCH(99)
-	-	3217	1.23	3350	5.17	γCH(85)
-	-	3211	5.41	3350	2.81	γCH(97)
-	-	3157	10.96	3280	18.31	γCH(99)
3065	3069	3079	16.52	3210	25.77	γCH(100)
1798	-	1708	364.45	1820	528.70	γOC(73)
-	-	1692	58.77	1803	23.73	γCC(26)+δHNC(10)
-	-	1688	23.91	1796	24.23	γCC(13)+δHNC(17)
-	-	1678	58.73	1786	42.56	γCC(31)+δHNC(13)
-	-	1657	0.16	1763	0.24	γCC(48)+δCCC(10)
-	1602	1625	61.82	1723	83.83	γCC(21)+δHNC(36)
1574	1577	1543	154.73	1649	124.17	γNC(13)+δHCC(45)+δCCC(12)
		1523	163.10	1628	100.08	γCC(14)+γNC(14)+δHCC(16)
1504		1511	9.59	1617	59.80	γCC(13)+δHCC(33)
		1497	16.20	1601	28.48	γCC(12)+δHCC(35)+δHCH(15)
		1494	5.25	1595	5.31	δHCH(52)
1454	1468	1453	211.50	1578	310.38	γOC(64)+γCC(13)+δOCO(10)
1382	1382	1377	83.87	1448	43.98	γCC(14)+γNC(34)+δHCC(10)
	-	1334	7.62	1433	77.76	γCC(12)
		1326	4.18	1389	7.64	τHCCC(26)
1303		1305	33.38	1369	1.94	γCC(43)
1274	-	1294	2.24	1350	0.31	γCC(16)+δHCC(48)
	1275	1275	0.25	1310	3.97	γCC(14)+δHCC(33)
1248	1234	1266	6.92	1304	3.35	γCC(21)+γNC(14)+δHCC(20)
	-	1206	4.27	1283	6.04	γCC(15)+δHCC(44)
1194	1194	1192	11.76	1238	6.04	γCC(10)+δHCC(51)
		1190	0.67	1235	27.51	δHCC(75)+τ HCCC(13)
1152	1160	1165	7.45	1211	13.90	γCC(11)
		1161	21.67	1195	1.96	γCC(15)+δHCC(11)
1099	-	1129	6.60	1183	33.88	γCC(41)+δHCC(21)
1088	-	1087	7.09	1156	15.69	γCC(17)+δCCC(24)+δHCC(30)
1069	1071	1072	23.38	1133	20.23	γCC(29)+γClC(12)+δCCC(30)
1042	1045	1018	0.28	1120	0.38	τ HCCC(75)+τ CCCC(12)
-	-	989	7.94	1092	0.46	τ HCCC(26)

Table 2: Contd.,						
-	-	983	3.83	1084	4.46	τ HCCC(69)
-	-	977	0.67	1061	0.09	τ HCCC(50)
-	-	962	6.83	1046	3.82	γOC(12)+γCC(32)
946	-	946	34.84	1025	12.80	τ HCCC(11)
939	-	927	5.27	1007	23.77	τ HCCC(48)
916	918	913	7.70	980	21.10	δ CCC(37)
-	-	901	6.89	961	11.49	τ HCCC(11)+δ OCOC(10)
891	890	882	7.14	950	5.12	τ HCCC(40)
845	835	818	10.91	881	6.67	δ OCO(14)+ δ OCOC(12)
-	-	787	28.61	862	47.03	τ HCCC(67)+ δ OCOC(13)
		783	30.62	851	39.61	τ HCCC(80)
765	762	775	84.65	827	71.78	δ CCC(10)+τ HNCC(20)
745		751	7.99	810	8.41	τ CCCC(43)
716	718	724	23.41	767	56.98	τ HNCC(13)+ τ CCCC(46)
-	-	701	28.62	744	35.77	γCC(10)+δ OCO(27)
692	-	691	8.59	729	9.93	γClC(15)+δ CCC(45)
667		642	24.70	676	21.00	γClC(15)+δ CCC(45)
636	604	629	6.68	665	16.30	δ CCC(31)
586		573	4.86	614	7.94	τ CCCN(15) + τ CCCC(10) +δ CCC(31)
553	-	553	5.55	590	6.15	τ CCCC(10) + γ ClCCC(13) + γ NCCC(10)
-	531	535	2.12	574	2.46	γ ClCCC(24) + γ NCCC(14)
		506	4.49	537	4.56	δ CCC(11) + δ NCC(15)
488		485	2.95	518	4.69	γClC(10)+δ CCC(12)
		477	6.30	509	5.90	γClC(12)+δ NCC(10)+γ ClCCC(14)
	-	465	1.98	499	1.56	τ CCCC(22)
	441	457	1.19	483	4.44	δ OCC(50)
	404	405	6.50	429	6.76	γClC(39)+δ ClCC(10)
	366	372	1.51	394	1.49	δ CCC(20)+δ ClCC(21)
	316	328	4.63	355	4.79	τ CCCN(16)+γ CLCCC(11)
		292	18.22	302	8.83	δ ClCC(17)+τ CCCN(14)
		269	18.55	278	26.07	γKO(21)+δ KOC(12)+γ ClCCC(12)
	-	257	18.07	258	8.86	γKO(37)
	237	238	2.73	250	4.17	δ CCC(10)+δ ClCC(32)+δ KOC (14)
	224	226	1.60	237	3.31	τ CCCC(10)+γ ClCCC(22)
	-	215	9.52	220	14.12	γKO(25)+δ CCC(12)
		176	8.14	175	10.96	δ OCC(11)+δ KOC(35)
	-	168	12.56	167	14.23	δ CCC(27)+δ ClCC(15)
		150	1.37	159	6.56	τ CCCC(60)+γ ClCCC(13)
	115	100	2.29	99	0.30	τ OCCC(35)
	92	90	14.38	83	5.51	τ CNCC(26)+τ KOCC(33)
	71	77	0.40	72	13.50	δ CNC(13)+δ CCC(15)+ τ OCCC(12)+γ CCCC(15)
	-	60	3.46	66	2.07	τ CCNC(23)+γ NCCC(15)
	-	50	4.54	51	4.76	τ OCCC(15)+τ CCCN(16)+ τ CNCC(11)+τ CCCC(17)+τ KOCC(13)
	-	31	3.38	36	3.81	δ CNC(18)+τ CCNC(18)+ τ KOCC(25)
		19	1.86	23	1.74	τ CNCC(22)+τ CNCC(14)+ τ CCCC(32)
						υ-stretching; $_{\delta}$-bending; τ-torsion. γ-Out of plane bending

Table 3: Experimental and Calculated Absorption Wavelenght (λ), Excitation State, Oscillator Strength (f), Electronic Absorption Value (eV) and Transition of K2DCPAPA by TD-DFT Method

Excitation	Singlet A	Cal. Wavelength (nm)	Wavelength (nm)	Oscillator Strength(f)	Electronic Absorption Value (eV)	Transition
Excited State 1						
85→86	0.67654	276	280.1	0.0094	4.426	HOMO ↔ LUMO
85→90	0.10447					HOMO ↔ LUMO+4
Excited state 2						
85→87	-0.11934		262.9	0.1215	4.7156	HOMO ↔ LUMO+1
85→89	0.59362					HOMO ↔ LUMO+3
85→90	-0.29379					HOMO ↔ LUMO+4
Excited State 3						
84 → 94	0.1946		250.4	0.0397	4.9506	HOMO-1↔LUMO+8
84 →95	0.12267					HOMO-1↔LUMO+9
85 →90	0.14439					HOMO↔LUMO+4
85 → 91	-0.13596					HOMO↔LUMO+5
85 → 92	-0.53224					HOMO↔LUMO+6
85 → 93	0.22899					HOMO↔LUMO+7

Table 4: The Calculated Thermodynamic Parameters of K2DCPAPA

Parameter	CAM-B3LYP	HF
Zero point vibrational energy(Kcal/Mol)	134.33462	142.26475
Dipole moment(Debye)	7.3681	7.8809
Rotational constant (GHz)	0.30522	0.30485
	0.28261	0.27012
	0.18336	0.17601
Rotational temperatures (Kelvin)	0.01465	0.01463
	0.01356	0.01296
	0.0088	0.00845
Entropy (Cal/Mol-Kelvin)		
Total	141.588	138.789
Translational	43.304	43.304
Rotational	34.274	34.36
Vibrational	64.01	61.125
Molar capacity at constant volume (Cal/Mol-Kelvin)		
Total	66.261	62.928
Translational	2.981	2.981
Rotational	2.981	2.981
Vibrational	60.299	56.967
Energy (KCal/Mol)		
Total	**145.556**	**153.047**
Translational	0.889	0.889
Rotational	0.889	0.889
Vibrational	143.779	151.27

Table 5: Chemical shift (^{13}C &^{1}H) for K2DCPAPA [δ (ppm)]

Atoms	CAM-B3LYP		HF		chemsoft
	Absolute Shielding	Chemical Shift	Absolute Shielding	Chemical Shift	Ultra
C2	70.35	129.63	77.08	122.90	127.2
C3	54.63	145.35	55.95	144.03	139.6
C4	71.79	128.20	79.22	120.76	118.7
C5	68.63	131.35	70.30	129.69	126.9
C6	79.91	120.08	85.06	114.92	120
C7	67.01	132.98	68.70	131.28	128.9
C8	21.51	178.48	19.59	180.40	175.4
C9	147.92	52.07	158.76	41.23	36.7
C13	53.44	146.55	56.84	143.14	139.6
C14	60.31	139.67	67.59	132.40	128.9
C15	69.67	130.31	73.04	126.95	126.9
C16	72.77	127.21	77.38	122.60	126
C17	70.00	129.99	72.79	127.19	126.1
C18	63.76	136.23	68.13	131.86	135.3
C19	773.61	-573.62	853.23	-653.24	-
C20	786.067	-586.08	863.548	-663.56	-
H21	24.0486	8.549	24.1873	8.4103	7.37
H22	24.7718	7.8258	24.8222	7.7754	6.76
H23	25.1131	7.4845	25.3032	7.2944	7.15
H24	24.6021	7.9955	24.6253	7.9723	7.37
H25	28.6538	3.9438	29.0479	3.5497	3.21
H26	28.2977	4.2999	28.8081	3.7895	4.1
H27	22.3814	10.2162	22.7244	9.8732	9.48
H28	24.5294	8.0682	24.7276	7.87	7.29
H29	24.5883	8.0093	24.818	7.7796	7.18
H30	24.3856	8.212	24.5449	8.0527	7.18

Table 6: Mulliken Atomic Charges of K2DCPAPA by CAM-B3LYP and HF Methods

Atoms	CAM-B3LYP	HF
K1	0.8488	0.8976
C2	-0.0510	-0.0888
C3	0.4406	0.4724
C4	0.2382	0.2387
C5	-0.0284	-0.0012
C6	-0.1375	-0.1621
C7	0.0430	0.0751
C8	1.0671	1.3080
C9	-0.0302	0.0329
O10	-0.9621	-1.0920
O11	-0.8941	-1.0537
N12	-0.8956	-0.8576
C13	0.4096	0.3806
C14	0.2338	0.2666
C15	-0.0699	-0.0749
C16	-0.0537	-0.0495
C17	0.0174	0.0268
C18	-0.1001	-0.0947
Cl19	-0.3210	-0.3376
Cl20	-0.3235	-0.3456
H21	0.0559	0.0536
H22	0.0478	0.0468

Table 6: Contd.,		
H23	0.0165	0.0146
H24	0.0240	0.0259
H25	-0.0050	-0.0196
H26	-0.0170	-0.0330
H27	0.3482	0.2788
H28	0.0455	0.0443
H29	0.0260	0.0230
H30	0.0267	0.0247

Table 7: Second Order Perturbation Theory Analysis of Fock Matrix in NBO Analysis

Donor(i)	Type	Acceptor(j)	Type	$E^{(2)a}$ KJ/mol)	E(j)-E(i)[b](a.u.)	F(i,j)[c](a.u.)
σ	C2-C3	σ*	C4-Cl19	5.22	0.97	0.064
σ	C2-C7	σ*	C3-C4	30.52	0.34	0.094
σ	C2-C9	σ*	C8-O11	3.72	0.85	0.054
σ	C3-C4	σ*	C5-C6	32.57	0.39	0.101
σ	C3-N12	σ*	C3-C4	2.17	1.48	0.048
σ	C4-C5	σ*	C3-C4	5.39	1.41	0.078
σ	C4-Cl19	σ*	C2-C3	2.7	1.4	0.055
σ	C5-C6	σ*	C2-C7	31.04	0.38	0.097
σ	C5-H22	σ*	C3-C4	4.82	1.21	0.069
σ	C6-C7	σ*	C2-C7	3.73	1.43	0.065
σ	C6-H23	σ*	C4-C5	4.12	1.23	0.064
σ	C7-H24	σ*	C2-C3	5.08	1.2	0.07
σ	C8-C9	σ*	C2-C7	2.18	0.76	0.04
σ	C8-O10	σ*	N12-H27	0.61	1.58	0.028
σ	C8-O11	σ*	C8-O11	2.68	0.69	0.042
σ	C9-H25	σ*	C2-C3	4.94	1.18	0.068
σ	C9-H26	σ*	C8-O11	4.94	1.09	0.067
σ	N12-C13	σ*	C2-C3	2.05	1.46	0.049
σ	N12-H27	σ*	C13-C14	6.2	0.71	0.066
σ	C13-C14	σ*	C14-C15	4.9	1.43	0.075
σ	C13-C18	σ*	C14-Cl20	5.97	0.96	0.068
σ	C14-C15	σ*	C13-C14	5.23	1.42	0.077
σ	C14-Cl20	σ*	C15-C16	2.56	1.45	0.054
σ	C15-C16	σ*	C14-Cl20	5.24	0.97	0.064
σ	C15-H28	σ*	C13-C14	4.59	1.22	0.067
σ	C16-C17	σ*	C17-C18	3.03	1.43	0.059
σ	C16-H29	σ*	C14-C15	4.19	1.23	0.064
σ	C17-C18	σ*	N12-C13	3.76	1.27	0.062
σ	C17-H30	σ*	C13-C18	4.24	1.23	0.065
σ	C18-H21	σ*	C13-C18	4.93	1.2	0.069
LP(1)	O10	π*	C8	9.02	1.6	0.108
LP(2)	O10	σ*	C8-O11	23.02	0.84	0.125
LP(1)	O11	π*	C8	11.05	1.58	0.118
LP(2)	O11	σ*	C8-O10	23.02	0.9	0.13
LP(1)	N12	σ*	C13-C18	4.61	0.94	0.061
LP(1)	Cl19	π*	C4	2.77	2.16	0.069

Table 7: Contd.,						
LP(2)	Cl19	σ*	C3-C4	4.86	1	0.062
LP(1)	Cl20	π*	C14	1.86	2.08	0.056
LP(2)	Cl19	σ*	C13-C14	4.62	1.01	0.061

Table 8: The Electric Dipole Moment (μ), Polarizability (α), and First Hyperpolarizability (β) of K2DCPAPA

	CAM-B3LYP		HF			CAM-B3LYP		HF	
	a.u.	esux10^{-24}	a.u.	esux10^{-24}		a.u.	esux10^{-33}	a.u.	esux10^{-33}
α_{xx}	186.22	27.60	170.36	25.25	β_{xxx}	93.08	804.14	86.80	749.86
α_{xy}	-38.85	-5.76	-37.50	-5.56	β_{xxy}	-135.76	-1172.84	-122.48	-1058.07
α_{yy}	214.65	31.81	202.69	30.04	β_{xyy}	50.87	439.50	42.43	366.51
α_{xz}	-3.67	-0.54	-4.73	-0.70	β_{yyy}	581.59	5024.32	541.55	4678.45
α_{yz}	-5.99	-0.89	-5.40	-0.80	β_{xxz}	23.74	205.07	22.43	193.73
α_{zz}	143.14	21.21	137.90	20.44	β_{xyz}	-48.43	-418.36	-42.90	-370.57
α_0	181.34	73.43	170.32	68.66	β_{yyz}	42.01	362.95	40.48	349.70
$\Delta\alpha$	62.36	9.24	56.11	8.32	β_{xzz}	-6.45	-55.72	-5.16	-44.58
μ_x	0.84		0.78		β_{yzz}	-8.80	-76.02	-6.62	-57.16
μ_y	-2.53		-2.42		β_{zzz}	43.38	374.75	36.25	313.16
μ_z	-1.13		-1.02		β_{tot}	635.23	5487.79	592.78	5121.03
μ	2.90		2.74						

Table 9 HOMO-LUMO Energy Value, Ionization Potential and Chemical Hardness of K2DCPAPA Method Calculated by B3LYP/6-31G(d,p) Method

Parameter		Parameter	
Energy (eV)			
EHOMO	-6.4962	Ionization potential (μ)	-3.53315
ELUMO	-0.5701	Chemical Hardness (η)	2.96307
ELUMO+1	0.5325	Softness (S)	0.16874
ELUMO+2	0.6438	Electronegativity (χ)	3.53315
ELUMO+3	0.9696	Electrophilicity index (w)	2.10645
ELUMO+4	1.1058		
ELUMO+5	1.5513		